A DUAL-OUTPUT POWER CONVERTER FOR LANDING GEAR ACTUATION USING MUTUAL POWER CIRCUIT COMPONENTS

Dr T Wijekoon*, Dr L Empringham*, Prof P W Wheeler*, Prof J C Clare*, C Whitley, J Melia** and G Towers****

** University of Nottingham, School of Electrical and Electronic Engineering, University Park, Nottingham, NG7 2RD, UK.*
Tel. +44 115 951 5591, Email: Pat.Wheeler@Nottingham.ac.uk
*** GE AVIATION, Mechanical Systems, Wobaston Road, Wolverhampton, WV9 5EW, UK.*

Keywords: *Electric Landing Gear, Electro Mechanical Actuator, BLDC drive, Hysteresis control*

Abstract

This paper describes the design, construction and testing of a dual-output power converter concept where only the large components, such as the DC link capacitor and heat-sink, are shared between two actuators which are used sequentially in the deployment of aircraft landing gear. This mutual component approach combines the advantages of dual-use power converters with the flexibility of one power converter per application. Practical results of the converter operating are presented for a range of test conditions in order to validate the simulation study.

1 Introduction

This paper introduces the dual-output Motor Control Unit (MCU) where large components, such as the DC link capacitor, filter-inductor, heat-sink, current sensors and control platform are shared between the output bridges. These two output bridges drive two separate motor loads which are operated sequentially. The design, construction and testing of the MCU are also discussed.

The ideas described in this paper are aimed at a future civil aircraft landing gear application where the converter will be used to control the extension and retraction of the undercarriage leg and the steering of the nose wheel on the ground. However, the concept could be used in a number of aircraft applications where sequential use of power converters is required.

The concept of the dual-output drive could be extended to include three or more sequential functions in future systems. For the system control in this application a Remote Electronic Unit (REU) will provide a high integrity command and monitoring system interfacing to various feedback position sensors and providing appropriate demands to the dual-output Motor Control Unit (MCU).

1.1 System Overview of the Nose Landing Gear

The outline of the system for the nose landing gear extension/ retraction and steering arrangement is shown in fig. 1. A single MCU drives two motor loads which are coupled with separate Electro Mechanical Actuators (EMA). One of the EMA is used for the extension and retraction operation. The second EMA is used for the steering of the nose wheel on the ground. The actuators are used sequentially so the power converter will feed only one load at a time.

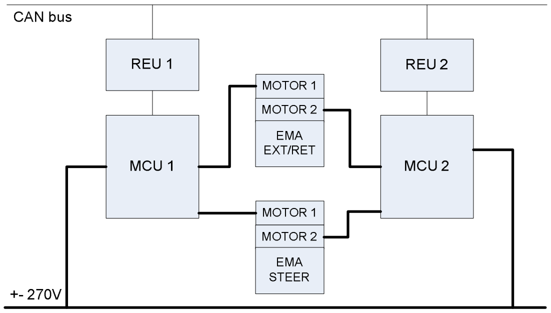

Fig. 1: System overview of the nose landing gear arrangement

The system has a dual modular redundancy for each EMA unit for the steering and Extension/Retraction operations. Each EMA has two motors mounted on the same shaft which are driven by two separate MCUs. Separate remote Electronic Units (REU) are allocated for each MCU. Each REU has command and monitoring modules which are interconnected by a CAN interface bus.

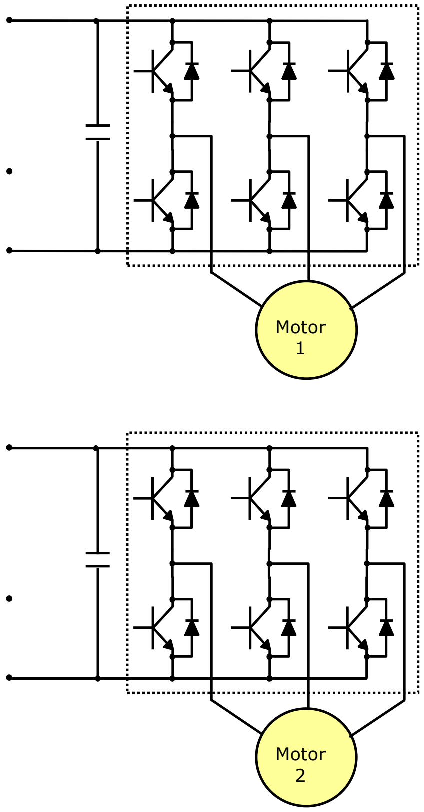

Fig. 2: A Single Power Converter for Each Load

2 Dual-output Motor Control Unit

The key power circuit components for possible power converter configurations for this application are shown in fig. 2 to fig. 4. The dual-output power converter configuration is a compromise solution between having one power converter per load (fig.2) and having a dual-use power converter with an output selection switch (fig. 3).

For the dual-use power converter, shown in fig. 3, an additional switch is used to switch the converter output between the two loads, this switch adds to the cost and size of the converter. If a solid sate switching component is used then this switch will also add to the losses of the power converter.

The components of a power converter which occupy size and weight are usually the DC link energy storage components and the heat-sinks for the power semiconductor devices. It is possible to design a power converter which will share these high size, cost and weight components, but still allow individual power semiconductor devices to be directly attached to each load. The power semiconductor devices are very small and light in comparison to these components, and hence this provides an alternative and potentially optimum solution, as shown in Fig. 4.

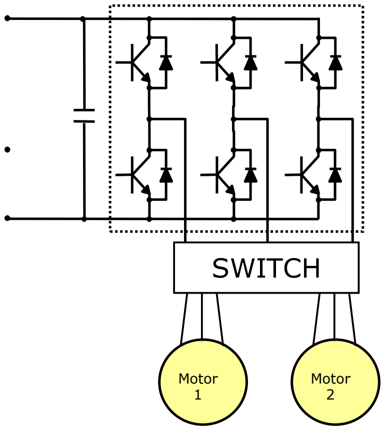

Fig. 3: A Dual-Use Power Converter

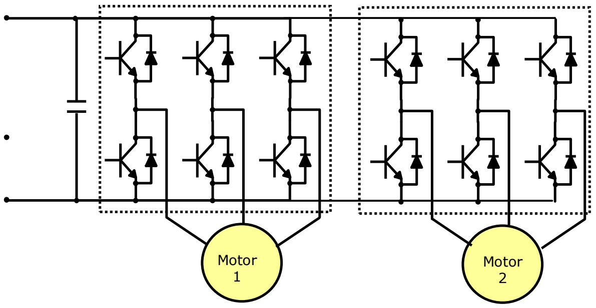

Fig. 4: A Dual-Output Power Converter with Mutual Components

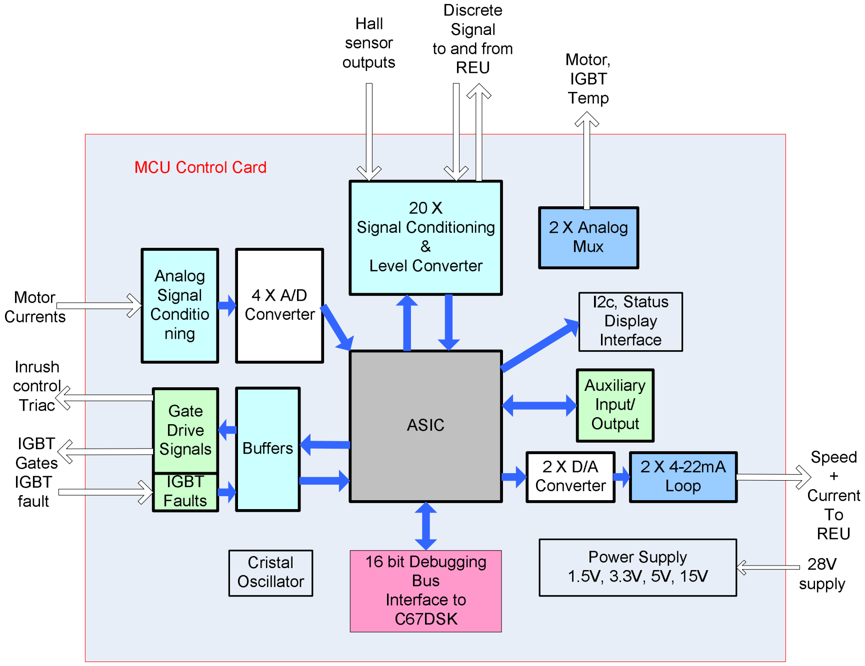

Fig. 6: Block diagram of the FPGA based Control Platform

The example given in this paper assumes a DC power system bus. However, the same principles can be applied to converters operating from an AC bus. The converters would have the added benefit of sharing the rectifier circuit. Most rectifier topologies employ heavy transforms [multi-phase rectifiers] or inductors [multiphase rectifiers or active rectifiers]. The sharing of the rectifier would lead to additional benefits in terms of reduced cost, weight and volume when a dual converter is compared to having a separate converter for each application.

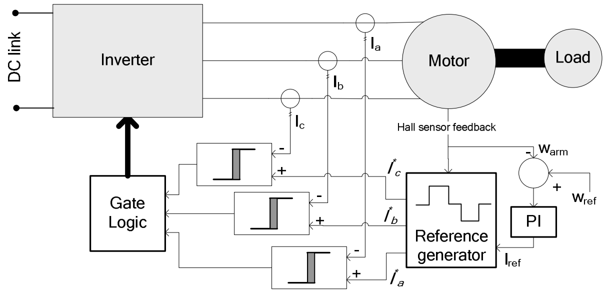

Fig. 5: Block diagram of the control and modulation of MCU

2.1 Modulation Technique

For this project a Brushless DC (BLDC) motor with a trapezoidal back e.m.f. is used. This type of machine has been chosen because it uses low cost sensors and has a high power/weight ratio. Both these features make for an optimized system design in this application and at the target power level. The BLDC motors are attached to the EMA and are controlled using a trapezoidal current control method [1][2]. Three Hall Effect sensors are mounted in the motor stator and can be used to extract the position information of the shaft [1][3]. This position information is translated into the commutation sequence and speed feedback for the motor control unit.

The trapezoidal motor currents are controlled using a hysteresis controller to achieve required torque of the motor. Fig. 5 shows the overall control and modulation scheme of the converter and machines.

Hysteresis based trapezoidal current control can be achieved with only one current sensor positioned in the dc link [4][5]. In this technique the motor currents are reconstructed using the measured dc link current.

In theory three motor currents are add up to zero in a delta connected motor. Therefore, measurements of only two motor currents are sufficient for the control of a delta connected BLDC motor [4].

However, in this project all three motor currents are measurements and used in order to improve the reliability of the drive. The third current measurement is used for validating the measurements and also used in case of any one of the sensors failed.

In this particular MCU arrangement these three current sensors are shared between two motor drives because the two motors are activated sequentially. This sharing is simply achieved by passing the cables for both motors through the same sensors. This arrangement provides further savings in the cost, size and complexity of the drive.

2.2 MCU Control Platform

Hysteresis band trapezoidal current control for a BLDC motor is simple to implement in a c Application Specific Integrated Circuit (ASIC) based control platform, without requiring any DSP or micro processor. BLDC motor control is well suited to this control implementation due to the absence of any complex mathematical calculations in the modulation process for the motor control. Therefore the size, cost and complexity of the control platform can be considerably reduced compared to control platforms motor drives which require sinusoidal waveforms. In this project a FPGA based control architecture is used for the MCU, which is shown in fig. 6. If a high number of MCUs were to be built the control can easily be implemented on an ASIC.

The DC link voltage and motor current measurements are digitized using on-board analog to digital converters. Signal conditioning units are incorporated for the Hall sensor feedback and discrete intercommunication signals from the REU, this signal conditioning is essential for operation in electrically noisy environments. The control platform also includes analog feedback signals using 4-20mA industrial standard current loop interfaces.

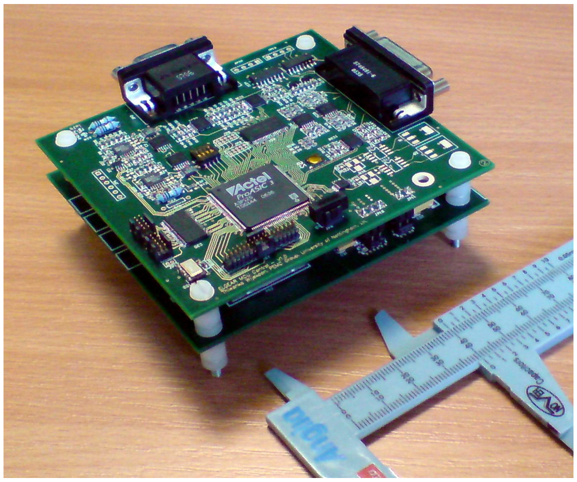

Fig. 7: The FPGA based control platform designed and developed for the Dual Converter MCU

An automatic pre-charge system for the dc link capacitor is included for the control of inrush current, as specified in the application specifications. A separate 16-bit interface bus is allocated for debugging of the system during the development and future improvement. A picture of the FPGA based control platform and interface hardware is shown in Fig. 7. The control platform has been designed as a set of small boards to match the overall form factor of the complete converter solution.

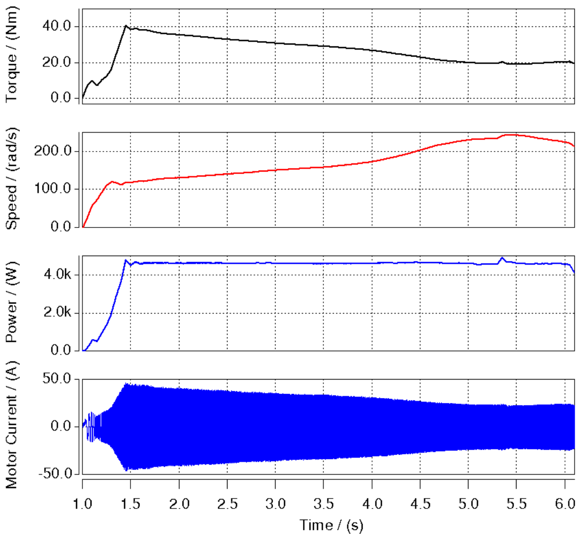

Fig. 8: Simulation results of the drive for retraction operation of the landing gear. (a) Torque, (b) Speed, (c) Power,

3 Simulation Results

Operation of the dual converter motor drive was simulated using Saber as the simulation tool. Estimated load conditions for a typical landing gear application in operation are used to emulate the motor load. Fig. 8 shows the waveform for the drive during the retraction operation of the landing gear, which is the worst case operation in terms of the motor drive power requirements.

This simulation study estimates the torque and speed limits for the motor drive. The maximum speed of the motor is limited to 2400rpm and the peak torque requirement for the motor is 40Nm. The maximum power required for the retraction operation had to be maintained at less than 5kW, the control this maximum power was achieved by adjusting the speed of the landing gear extension operation.

The MCU has been developed to operate from a DC bus, although the same approach could be used with an AC power system bus. Supply current waveforms from the +-270V dc bus have to be filtered in order to comply with required standards [6]. The dc link filter are incorporated within this multi-drive MCU and these components are obviously shared between both motor drive loads to minimize the size, weight and volume of the converter.

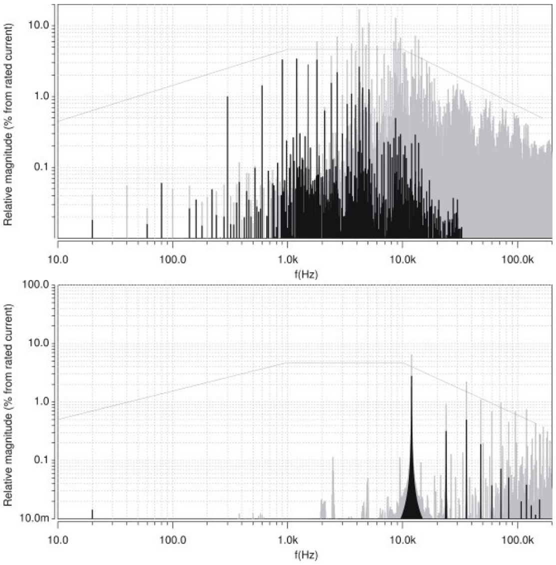

Fig. 9: Fourier spectrum of the +-270V supply current. (a) 2500rpm, 40Nm load. (b) 10rpm, 40Nm load.

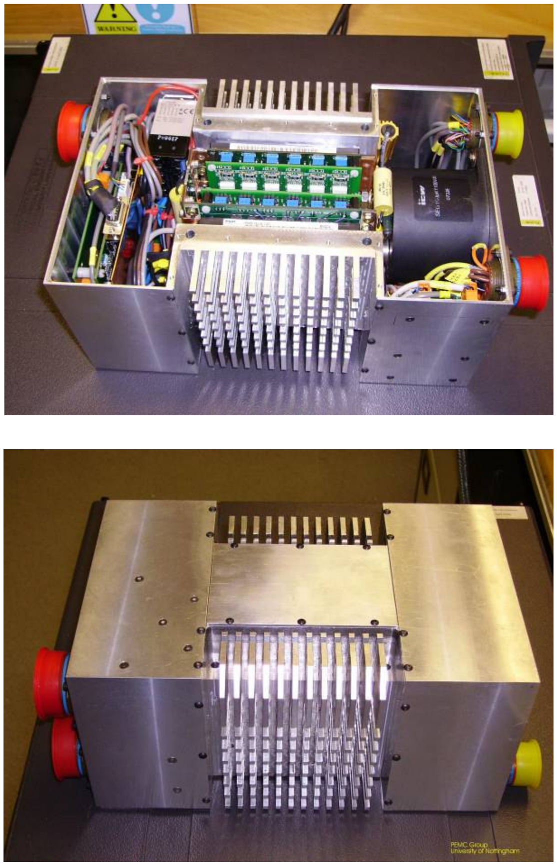

Fig. 10: Prototype hardware unit of the dual-output output MCU

Fig. 9 shows the Fourier spectrums of the +-270V bus current for two extremes of the operating speeds, both at the peak load of 40Nm. The maximum allowable limits specified in the standards [6] are shown in horizontal lines. The darker waveforms indicate the filtered current spectrum whilst the lighter waveforms show the unfiltered current spectrum. It can clearly be seen that the waveforms meet the standard under both these worst case operating conditions.

3.1 Experimental Results

Fig. 10 shows the prototype hardware unit of the dual-output MCU, which was built with the intention of demonstrating the minimization of volume and weight. AutoCAD Computer Aided Design software was used for the designing the casing and the mechanical optimization component arrangements.

The prototype heat-sink was milled out using block of aluminum according to the required thermal mass for heat dissipation within the drive hardware. The thermal dissipation requirement for the heat-sink was estimated using analytical methods which give the power loss of the drive under the worst case operating conditions.

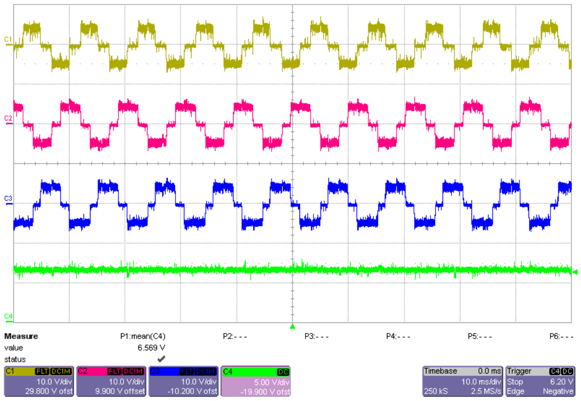

Fig. 11: Typical three-phase motor currents and the filtered dc link current

The pin cooling surface arrangement, shown in fig. 10, was chosen mainly to remove the unwanted material and also to reduce the complexity of the milling operation. However, with the use of thermodynamic software analysis a more optimum cooling arrangement can be achieved, which potentially could further reduce the weight of the MCU.

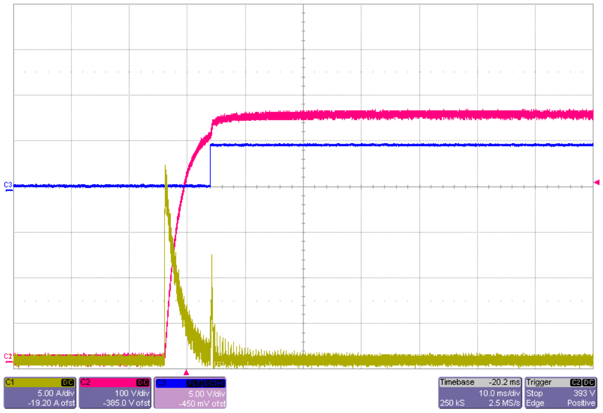

Fig. 12: Operation of the inrush limiting pre-charge circuit arrangement.

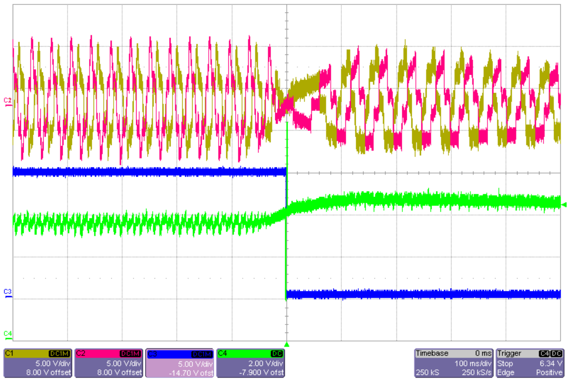

Fig. 13: Current, speed demand and actual speed waveforms for a speed reversal

The three motor currents and filtered +-270V dc bus current of the MCU controlling the motor at constant speed and load torque is shown in fig. 11. The three motor currents are trapezoidal in shape and 120° electrically apart each other, as expected.

The inrush current of the MCU was limited by employing a pre-charge circuit. The pre-charge circuit comprises of a Triac in parallel with a resistor. The dc link bus voltage is monitored and compared with set values in order to operate the Triac at particular dc link voltage level. The resistor has been chosen to ensure that the inrush current meets the requirements of the application.

The voltage and current waveforms of +-270V dc bus during the start-up is shown in fig. 12. The Triac operates when the total magnitude of the DC link voltage is above 500V and bypasses the pre-charging resistors. Once this resistor has been bypassed the MCU is available for operation when required. The blue color waveform in fig. 12 shows the gate logic signal to the Triac. For this application the charging resistors have been selected to limit the inrush current 23A

As a demonstration of the operation of the MCU, a speed reversal of the motor under constant torque operation is shown in fig. 13. The top waveforms are the three-phase motor currents. The blue color waveform indicates the speed demand and the green color waveform represents the speed feedback signal, reversed in regards to the reference.

Conclusions

This paper has demonstrated the design, construction and operation of an example of a dual-output power converter with mutual large power circuit components. This proposed power converter structure has the benefits of sharing the large or expensive components between converters whilst maintaining an output inverter bridge for each load. For higher power converters the benefits of this solution will be even greater, for example as a replacement of the concept of a dual use converter for ECS and engine start applications.

This paper has demonstrated that this type of advanced dual-output power converter is achievable and practical for aerospace some applications.

References

[1] Pillay P and Krishnan R**.** Modeling, simulation and analysis of permanent-magnet motor drives, Part II: The brushless DC motor drive. *IEEE Transactions on Industry Applications,* Vol. 25, No. 2, pp 274-278, 1989.

[2] Nam K Y, Lee W T, Lee C M and Hong J P. Reducing torque ripple of brushless DC motor by varying input voltage. *IEEE Transactions on Magnetics,* Vol. 42, No. 4, pp 1307-1310, 2006.

[3] Holmes D G and Lipo T A, *Pulse Width Modulation for Power Converters: Principles and Practice*, Number ISBN: 0-471-20814-0. Wiley.

[4] Dixon j W and Leal I A. Current Control for AC Motor Drives Using a Single DC-Link Current Sensor and Measurement Voltage Vectors, *IEEE Transactions on Power Electronics,* Vol. 17, No. 2, 2002.

[5] Kim H and Jahns T M. Current control strategy for brushless dc motors based on a common DC signal. *IEEE Transactions on Industry Applications,* Vol. 42, No. 6, 2006.

[6] DDIS. *Aircraft Electric Power Characteristics*: MIL-STD-704F, March 2004.

[7] Schafmeister F and Kolar J. Analytical calculation of the conduction and switching losses of the conventional matrix converter and the sparse matrix converter, *Proc. of IEEE Applied Power Electronics Conference*, vol. 2, pp. 875 - 881, 2005.

[8] Abraham L and Reddig M. Determination of switching losses in IGBTs by loss-summation method, *Proc. of IEEE Industry Applications Society Annual Meeting*, vol. 2, pp. 1061 - 1068,1995.

Copyright Statement